Stratospheric ozone depletion reduces ocean carbon uptake and enhances ocean acidification

Andrew Lenton,[1] Francis Codron,[2] Laurent Bopp,[3] Nicolas Metzl,[1] Patricia Cadule,[3] Alessandro Tagliabue,[3] and Julien Le Sommer[4]

Received 17 March 2009; revised 22 April 2009; accepted 19 May 2009; published 20 June 2009.

[1] Observational and atmospheric inversion studies find that the strength of the Southern Ocean carbon dioxide (CO_2) sink is not increasing, despite rising atmospheric CO_2. However, this is yet to be captured by contemporary coupled-climate-carbon-models used to predict future climate. We show that by accounting for stratospheric ozone depletion in a coupled-climate-carbon-model, the ventilation of carbon rich deep water is enhanced through stronger winds, increasing surface water CO_2 at a rate in good agreement with observed trends. We find that Southern Ocean uptake is reduced by 2.47 PgC (1987–2004) and is consistent with atmospheric inversion studies. The enhanced ventilation also accelerates ocean acidification, despite lesser Southern Ocean CO_2 uptake. Our results link two important anthropogenic changes: stratospheric ozone depletion and greenhouse gas increases; and suggest that studies of future climate that neglect stratospheric ozone depletion likely overestimate regional and global oceanic CO_2 uptake and underestimate the impact of ocean acidification. **Citation:** Lenton, A., F. Codron, L. Bopp, N. Metzl, P. Cadule, A. Tagliabue, and J. Le Sommer (2009), Stratospheric ozone depletion reduces ocean carbon uptake and enhances ocean acidification, *Geophys. Res. Lett.*, *36*, L12606, doi:10.1029/2009GL038227.

1. Introduction

[2] The Southern Ocean (SO; south of 40°S) plays an important role mitigating climate change, acting as a significant sink for atmospheric carbon dioxide (CO_2) that is observationally estimated to account for >40% of the total annual oceanic uptake [*Takahashi et al.*, 2009]. Atmospheric CO_2 primarily enters the ocean via air-sea fluxes, which are principally a function of the gradient between the partial pressures of CO_2 (pCO_2) in the surface ocean and atmosphere ($pCO_{2atm} - pCO_{2ocean} = \Delta pCO_2$) and wind speed (piston velocity [e.g. *Wanninkhof*, 1992]). Increasing atmospheric CO_2 levels should, a priori, enhance ΔpCO_2 and hence CO_2 uptake accordingly. However, recent SO observational studies have shown that the value of surface water pCO_2 has increased at a similar or a slightly faster rate than the mean atmospheric growth rate over recent decades [*Metzl*, 2009; *Takahashi et al.*, 2009]. This is consistent with inversions of observed atmospheric CO_2 concentrations that show that the SO CO_2 sink is not increasing [*Le Quéré et al.*, 2007]. In contrast, coupled-climate-carbon models (CCCMs), used to predict future interactions between carbon and climate, predict a strengthening SO CO_2 sink [e.g., *Crueger et al.*, 2008]. That CCCMs cannot reproduce recent observed changes is a shortcoming that must be addressed if we are to have confidence in their projections, especially at regional scales.

[3] Ocean-carbon models that are driven by atmospheric observations suggest the reduction in air-sea CO_2 fluxes results from increased wind driven ocean ventilation that enhances the ventilation of carbon-rich deepwater. This increases carbon concentration in the upper ocean thereby reducing the gradient between the atmosphere and ocean leading to a decreased CO_2 uptake [*Le Quéré et al.*, 2007; *Lenton and Matear*, 2007], although the precise mechanisms have been recently questioned [*Böning et al.*, 2008]. Stronger SO winds are part of the surface signature of the Southern Annular Mode (SAM), which is a pattern of atmospheric variability that is characterized in its positive phase by a poleward shift of the westerlies. Over recent decades, the SAM has exhibited a strong upward trend [*Marshall*, 2003] that is primarily driven by increased greenhouse gas concentrations (GHGs) and stratospheric ozone depletion [*Arblaster and Meehl*, 2006], although the dynamical mechanism by which stratospheric anomalies propagate to the lower atmosphere remains unresolved [*Song and Robinson*, 2004].

[4] Climate only models (i.e. non-carbon coupled) that include stratospheric ozone depletion, potentially even underestimating its response [*Perlwitz et al.*, 2008; *Son et al.*, 2008], simulate a stronger SAM and increased SO winds speeds than those driven by GHGs alone [*Cai and Cowan*, 2007]. However these models do not explicitly represent the interactions between atmospheric dynamics and ocean biogeochemistry and thus are unable to address the impact of stratospheric ozone deletion on carbon uptake, ocean biology and ocean acidification. Current CCCMs, that explicitly represent the interactions between climate and the carbon cycle, do include the increase in GHGs, but stratospheric ozone depletion is neglected.

[5] In this study we include stratospheric ozone depletion in a CCCM and demonstrate that it drives a significant decrease in both regional and global ocean CO_2 uptake. We demonstrate that by including ozone depletion observations we can reconcile CCCM predictions with recent observations, as well as quantifying its impact on carbonate chemistry, biological productivity, ocean acidification and regional and global CO_2 uptake. To this end we use ensemble simulations of the IPSL-CM4-LOOP coupled-climate carbon model [*Friedlingstein et al.*, 2006] driven

[1] LOCEAN, IPSL, UPMC, MHNH, IRD, CNRS, Paris, France.
[2] LMD, IPSL, UPMC, X, ENS, CNRS, Paris, France.
[3] LSCE, IPSL, CEA, UVSQ, CNRS, Gif-sur-Yvette, France.
[4] LEGI, UJF, INPG, CNRS, Grenoble, France.

0094-8276/09/2009GL038227

with and without stratospheric ozone depletion in the period between 1975 and 2004.

2. Methods

[6] The IPSL-CM4-LOOP 3D prognostic climate-carbon-coupled-model [*Marti et al.*, 2006] comprises the (1) Laboratoire de Météorologie Dynamique atmospheric model (LMDZ4) [*Hourdin et al.*, 2006], (2) Organizing Carbon and Hydrology in Dynamic Ecosystems (ORCHIDEE) [*Krinner et al.*, 2005] land use carbon cycle model, (3) ORCALIM2 ocean and sea ice model [*Timmerman et al.*, 2005], and (4) the Pelagic Interaction Scheme for Carbon and Ecosystem Studies (PISCES) [*Aumont and Bopp*, 2006] marine biogeochemical model (see auxiliary material for more detail).[1]

[7] To avoid a large discontinuity in CO_2 emissions, land use changes from 2000–2004 were scaled by observed values [*Houghton and Hackler*, 2002]. Concentrations of non-CO_2 greenhouse gases (CFC11, CFC12, CH_4, SO_4) and aerosols are included [*Boucher and Pham*, 2002], the solar forcing was held constant at 1365 W/m^2 and the impact of volcanic eruptions not considered.

[8] To ensure a robust result and to test the sensitivity of our results to different atmospheric conditions we performed two ensembles of 5 control (O_3clim) and 5 test (O_3hole) cases with and without stratospheric ozone depletion respectively. All members were started with identical initial conditions for the ocean, land and sea-ice. The initial state in the atmosphere was then changed by several days for each ensemble pair.

[9] In the O_3clim simulations, ozone values were based on a climatology [*Keating and Young*, 1985]. In the O_3hole simulations, we augmented this climatology with a linear decrease in the polar lower stratosphere from 1975 to 2000. We adjust the latitude-pressure structure of the trend, and its seasonal magnitude, to be consistent with observations [*Randel and Wu*, 2007]. After 2000, the amplitude of ozone depletion is held constant except for seasonal variation.

3. Results and Discussion

[10] The SAM trend computed from O_3hole shows very little difference between 1975 and 1986, relative to O_3clim. In the period 1987 onwards, O_3hole has a marked maximum in the austral spring/summer and a strong positive trend (+0.25 ± 0.06 σ/decade; σ = standard deviation) that is consistent with observations (+0.21 σ/decade) [*Marshall*, 2003]. Conversely, O_3clim exhibits almost no SAM trend (−0.09 ± 0.09 σ/decade) and no seasonality over the same period. Initially, there are only small differences in wind stress between ensembles, but from 1987 the differences in wind stress between O_3hole and O_3clim become progressively larger in time. Westerlies are shifted polewards and zonally averaged wind stresses increase by up to 60% locally (Figure 1a).

[11] Initially, the similarity in wind stresses leads to no significant difference in supply of deepwater to the upper ocean and hence no significant difference in ΔpCO_2 (air-sea

[1]Auxiliary materials are available in the HTML. doi:10.1029/2009GL038227.

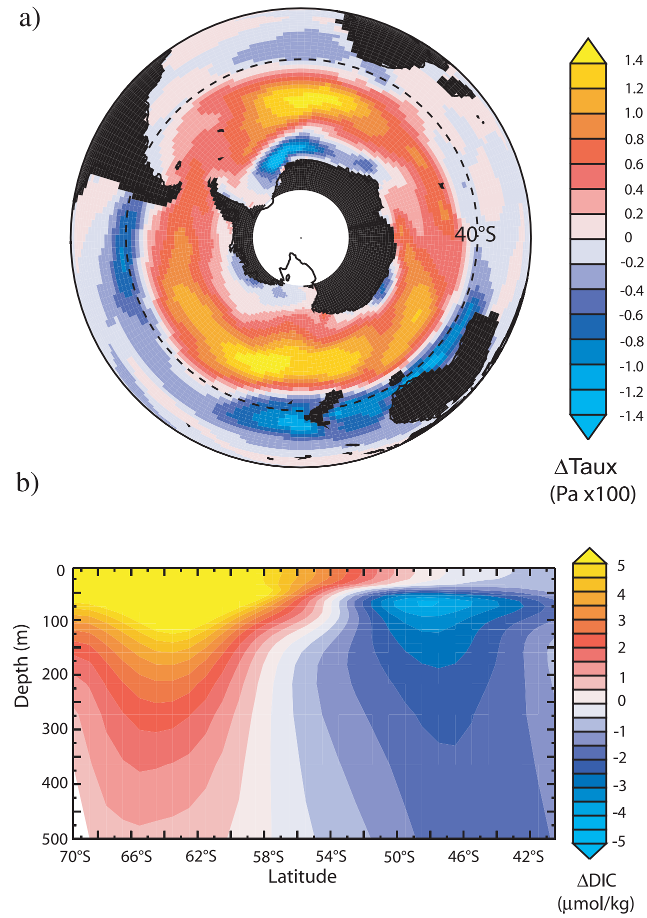

Figure 1. (a) Zonal wind stress difference between O_3hole and O_3clim, 1994–2004 average (Pa x100; positive is clockwise). (b) Zonal-mean difference in dissolved inorganic carbon (DIC) concentrations between O_3hole and O_3clim (μmol/kg; 1994–2004) in response to Figure 1a.

pCO_2 gradient) between O_3hole and O_3clim (Figure 2). However, as the wind stress increases in O_3hole, there is an enhancement of the upward and equatorward transport of carbon-rich deep water that increases surface water dissolved inorganic carbon (DIC >6 μmol/kg south of 60°S; Figure 1b) and hence pCO_2. This increase in surface water pCO_2 in response to stratospheric ozone depletion leads to a reduction in ΔpCO_2. The associated increase in alkalinity compensates partly for the increase in surface water pCO_2, while the very small increase in primary production (<2%; 1975–2004) likely plays little role. Without stratospheric ozone depletion, ΔpCO_2 increases, which is consistent with a strengthening gradient in response to CO_2 emissions alone.

[12] An increased vertical supply of limiting nutrient (iron) to surface waters should increase net primary productivity (NPP) [*de Baar et al.*, 2005] and hence act to lower oceanic pCO_2 The low sensitivity of net primary production (NPP) to increased iron (<2%) is controlled by a concomitant increase in the phytoplankton iron demand (expressed as the amount of iron required to fix one unit of CO_2, Fe/C). The iron demand increases with a greater seawater iron concentration [*Sunda and Huntsman*, 1997] and as a result of the increased diatom dominance that

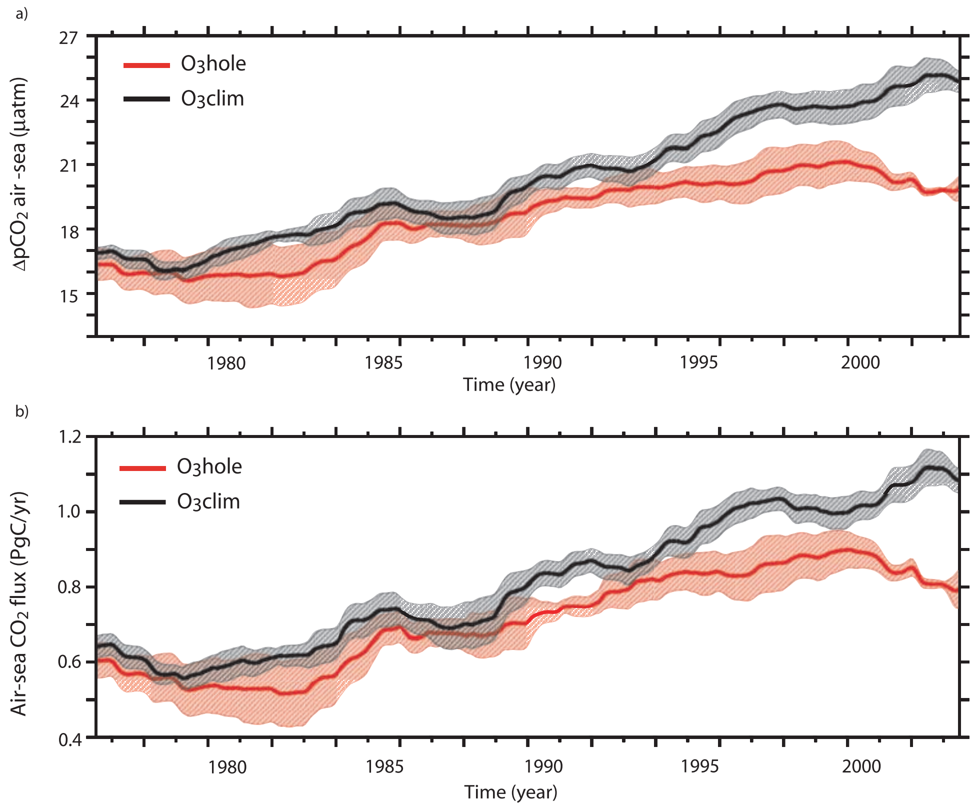

Figure 2. (a) Spatially averaged ΔpCO_2 (south of 40°S), showing that accounting for stratospheric ozone depletion (O_3hole) reduces ΔpCO_2 (relative to O_3clim), in response to increased upper ocean carbon concentration (Figure 1b). (b) Integrated air to sea CO_2 flux (south of 40°S) showing stratospheric ozone depletion (O_3hole) significantly reduces CO_2 uptake (relative to O_3clim), and is strongly correlated with changes in ΔpCO_2. The values of ΔpCO_2 and CO_2 fluxes represent the ensemble mean, while the shaded area represents the standard error of the mean. CO_2 fluxes and ΔpCO_2 are smoothed with 36-month running mean filters.

follows the addition of iron [*de Baar et al.*, 2005]. The efficiency with which iron can fuel NPP is therefore depressed and NPP only increases moderately in O_3hole. Importantly, the amount of chlorophyll associated with a given quantity of phytoplankton carbon (the chlorophyll to carbon ratio) is also greater with lesser iron limitation, which suggests that chlorophyll and NPP can become decoupled in response to changes in vertical nutrient supply. This would suggest that satellite observations of elevated chlorophyll-a in response to increased winds [*Lovenduski and Gruber*, 2005] need to account for the associated variability in phytoplankton chlorophyll to carbon ratios, which may actually drive a weak biological response.

[13] Circumpolar observations of oceanic pCO_2 growth rate collected during the SO austral winter, south of 50°S (and south of 40°S regionally), thereby avoiding the spatial heterogeneity of summer growing season and CO_2 solubility changes, show that surface waters have increased at a similar or a slightly faster rate (2.1 ± 0.6 μatm/year; Table 1) than the mean atmospheric growth rate over the same period (1.7 μatm/year; Table 1) [*Takahashi et al.*, 2009; *Metzl*, 2009]. This region (circumpolar south of 50°S) corresponds to the region of the largest changes in the supply of carbon-rich deepwater to the upper ocean (Figure 1b) and is characterised by deep winter mixing and low productivity during the austral winter. We see when stratospheric ozone depletion is neglected (O_3clim), the oceanic growth rate is significantly lower (1.1 ± 0.1 μatm/yr; Table 1) than the atmospheric growth rate (1.9 μatm/yr; Table 1), in discord with observations. Conversely, by including stratospheric ozone depletion (O_3hole) we find that the oceanic surface water pCO_2 growth rate increases at a similar rate (2.0 ± 0.2 μatm/yr; Table 1) to that of the atmosphere (2.0 μatm/yr; Table 1), in good agreement with observations.

[14] Mirroring the changes in ΔpCO_2, there is initially little difference in integrated SO CO_2 fluxes between O_3clim and O_3hole (each a sink of ~0.6 PgC/yr; Figure 2). However, as the wind stress increases, there is a marked reduction in SO CO_2 uptake in O_3hole, relative to O_3clim (wherein SO CO_2 uptake continues to increase; Figure 2b). The linear trends in SO CO_2 uptake are significantly different ($p < 0.01$; 1987–2004; see auxiliary material) and cumulative SO CO_2 uptake is reduced by 2.47 PgC in O_3hole. The strong correlation ($R > 0.99$) between air-sea CO_2 fluxes and ΔpCO_2 demonstrates the importance of changes in oceanic pCO_2 rather than increased wind speed, which would act to increase SO CO_2 uptake.

[15] Inversions of atmospheric observations in the region south of 45°S show the SO CO_2 sink is not increasing (−0.03 PgC/yr/decade; 1981–2004) [*Le Quéré et al.*, 2007]. When stratospheric ozone depletion is included (O_3hole) we also find that the strength of SO CO_2 sink (in absolute terms) is also not increasing, at a rate very similar to that reported (−0.02 PgC/yr/decade; 1994–2004)

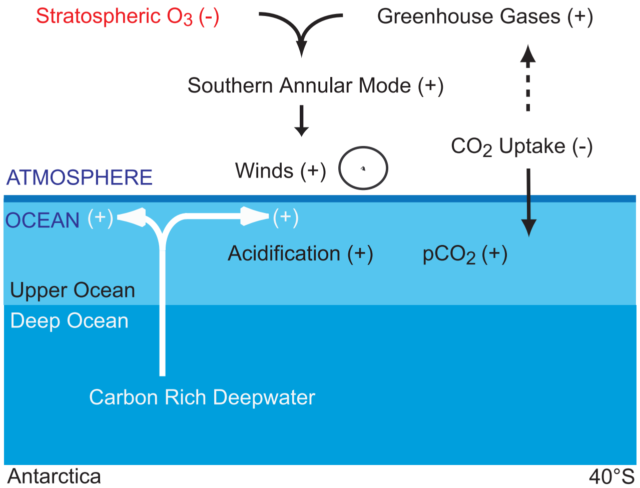

Figure 3. The response of the Southern Ocean to stratospheric ozone depletion. Stratospheric ozone depletion in conjunction with greenhouse gases drives a stronger SAM, which increases the strength of westerly winds driving enhanced ventilation of carbon rich deepwater. Enhanced ventilation increases the pCO_2 in ocean surface waters, thereby reducing the ΔpCO_2 and air-sea CO_2 fluxes. Reduced uptake leads to a small increase in atmospheric CO_2 concentration. Associated with the enhanced ventilation of carbon rich deepwater is an increase in ocean acidification. Positive (+) represents an increase/strengthening and negative (−) represents a decrease/weakening of a given process.

over the same region. The global oceanic CO_2 sink is also impacted and cumulative uptake declines by 2.33 PgC in O_3hole (relative to O_3clim 1987–2004), highlighting the impact of stratospheric ozone depletion on global ocean carbon uptake. As a consequence of this reduction in global oceanic CO_2 uptake, the atmospheric CO_2 growth rate increases in O_3hole (Table 1) and elevates atmospheric CO_2 concentrations (by 1.2 ppm; 1975–2004) thereby quantifying the weak positive feedback of stratospheric ozone depletion on atmospheric CO_2 levels.

[16] Despite reduced CO_2 uptake, enhanced ventilation of carbon rich deep water in response to stratospheric ozone depletion accelerates the rate of ocean acidification. As the carbon content of the upper ocean increases there is a concomitant decrease in seawater pH or acidification. Ocean acidification, in conjunction with rising ocean carbon concentrations, will impact on key SO calcifying marine organisms (e.g. pteropods and coccolithophorids) by modifying their ability to form calcium carbonate shells [*Iglesias-Rodriguez et al.*, 2008; *Raven et al.*, 2005]. One of the key carbon parameters in response to acidification is the aragonite saturation state (Ω_A), which impacts rates of calcification [*Langdon and Atkinson*, 2005; *Riebesell et al.*, 2000]. To quantify the impact of stratospheric ozone depletion on the aragonite saturation horizon (ASH; $\Omega_A = 1$, i.e., the transition depth between over- to under-saturated) and surface ocean pH, the mean differences south of 60°S in SO were calculated in the period 1994–2004 (corresponding to the largest changes in CO_2 uptake). The total change (O_3hole) in ASH was 55 m (1994–2004) and 40% of this shallowing was in response to stratospheric ozone depletion alone, which represents 7% of the total change in ASH that has occurred since the preindustrial [*Orr et al.*, 2005]. The total change in mean surface water pH was 0.02 (1994–2004; O_3hole) with 50% due to stratospheric ozone depletion, which represents 10% of the change since the preindustrial [*Raven et al.*, 2005]. These results demonstrate that anthropogenic changes present in O_3clim due to anthropogenic CO_2 are enhanced when stratospheric ozone depletion is included and suggests that high latitude SO surface waters may become understaturated with respect to aragonite ($\Omega_A < 1$) sooner than was previously predicted [*Orr et al.*, 2005].

[17] Recent studies suggest that increased mesoscale eddy activity associated with greater winds reduces the sensitivity of the response of SO overturning circulation to changes in Southern Hemisphere winds [e.g., *Böning et al.*, 2008]. The response of CO_2 fluxes to the combined impact of changing deep-water ventilation and eddy effects is unclear and remains to be assessed by fully eddy-resolving ocean-carbon models. Nevertheless, we believe that that the main results of this study, using a non-eddy resolving model, are robust because (1) eddy resolving models do show elevated winds cause an increase in deep-water ventilation consistent with our study and (2) the reduced vertical supply of carbon due to eddy advection could be compensated for by enhanced eddy diffusion. Our ability to reproduce the observed SO trends in oceanic pCO_2 and CO_2 provides further confidence in our results.

4. Conclusion

[18] We have demonstrated how upper atmosphere changes impact the ocean by increasing surface water pCO_2 to be consistent with observations. The subsequent reduction in ΔpCO_2 translates to a significant reduction in regional and global air-sea CO_2 fluxes; moreover, despite this reduced CO_2 uptake there is an increase in the rate of ocean acidification (Figure 3). Our results suggest that

Table 1. Austral Winter SO Seawater pCO_2 Trends Calculated From Circumpolar and Regional Observations, and Ensemble Simulations With and Without Stratospheric Ozone Depletion[a]

	pCO_2ocean (μatm/yr)	pCO_2atm (μatm/yr)	Period	Southern Ocean Region (<50°S)
Observations [*Metzl*, 2009]	2.1 ± 0.3	1.7	1991–2000	Indian Sector
Observations [*Takahashi et al.*, 2009]	2.1 ± 0.6	1.7	1986–2007	Circumpolar
O_3hole	2.0 ± 0.2	2.0	1986–2004	Circumpolar
O_3clim	1.1 ± 0.1	1.9	1986–2004	Circumpolar

[a]Trends are from south of 50°. The uncertainty in simulations represents the standard error of the mean. Atmospheric pCO_2 concentration is expressed in μatm/yr, the same value as observed trends of molar fraction, xCO_2 (ppm/yr). O_3hole are observations with stratospheric ozone depletion, and O_3clim are ensemble simulations without stratospheric ozone depletion.

predictions of future climate that do not account for stratospheric ozone depletion likely overestimate regional and global oceanic CO_2 uptake and underestimate ocean acidification. In the future, stratospheric ozone recovery and increased GHGs will be the dominant SAM drivers impacting SO winds [*Arblaster and Meehl*, 2006; *Son et al.*, 2008]; our study demonstrates the importance of including stratospheric ozone in both reproducing recent observations and predicting the future evolution of the ocean carbon sink.

[19] **Acknowledgments.** We thank Pierre Friedlingstein, the French National Computing Centre (IDRIS/CCRT) and Program LEFE/Cyber, and the European Integrated Project CARBOOCEAN 511176.

References

Arblaster, J. M., and G. A. Meehl (2006), Contributions of external forcings to Southern Annular Mode trends, *J. Clim.*, *19*, 2896–2905.

Aumont, O., and L. Bopp (2006), Globalizing results from ocean in situ iron fertilization studies, *Global Biogeochem. Cycles*, *20*, GB2017, doi:10.1029/2005GB002591.

Böning, C. W., et al. (2008), The response of the Antarctic Circumpolar Current to recent climate change, *Nat. Geosci.*, *1*, 864–869.

Boucher, O., and M. Pham (2002), History of sulfate aerosol radiative forcings, *Geophys. Res. Lett.*, *29*(9), 1308, doi:10.1029/2001GL014048.

Cai, W., and T. Cowan (2007), Trends in Southern Hemisphere circulation in IPCC AR4 models over 1950–1999: Ozone depletion verus greenhouse forcing, *J. Clim.*, *20*, 681–693.

Crueger, T., et al. (2008), Ocean dynamics determine the response of oceanic CO_2 uptake to climate change, *Clim. Dyn.*, *31*, 151–168.

de Baar, H. J. W., et al. (2005), Synthesis of iron fertilization experiments: From the Iron Age in the Age of Enlightenment, *J. Geophys. Res.*, *110*, C09S16, doi:10.1029/2004JC002601.

Friedlingstein, P., et al. (2006), Climate-carbon cycle feedback analysis: Results from the C4MIP model intercomparison, *J. Clim.*, *19*, 3337–3353.

Houghton, R. A., and J. L. Hackler (2002), Carbon flux to the atmosphere from land-use changes: 1850 to 1990, *Rep. NDP-050/R1*, Carbon Dioxide Inf. Anal. Cent., Oak Ridge Natl. Lab., U.S. Dep. of Energy, Oak Ridge, Tenn.

Hourdin, F., et al. (2006), The LMDZ4 general circulation model: Climate performance and sensitivity to parametrized physics with emphasis on tropical convection, *Clim. Dyn.*, *27*, 787–813.

Iglesias-Rodriguez, M. D., et al. (2008), Phytoplankton calcification in a high-CO_2 world, *Science*, *320*, 336–340.

Keating, G. M., and D. F. Young (1985), Interim reference models for the middle atmosphere, in *Handbook for the Middle Atmosphere Programme*, vol. 16, pp. 205–229, ICSU Sci. Comm. on Sol. Terr. Phys., Univ. of Ill., Urbana.

Krinner, G., N. Viovy, N. de Noblet-Ducoudré, J. Ogée, J. Polcher, P. Friedlingstein, P. Ciais, S. Sitch, and I. C. Prentice (2005), A dynamic global vegetation model for studies of the coupled atmosphere-biosphere system, *Global Biogeochem. Cycles*, *19*, GB1015, doi:10.1029/2003GB002199.

Langdon, C., and M. J. Atkinson (2005), Effect of elevated pCO_2 on photosynthesis and calcification of corals and interactions with seasonal change in temperature/irradiance and nutrient enrichment, *J. Geophys. Res.*, *110*, C09S07, doi:10.1029/2004JC002576.

Lenton, A., and R. J. Matear (2007), The role of the Southern Annular Mode (SAM) in Southern Ocean CO_2 uptake, *Global Biogeochem. Cycles*, *21*, GB2016, doi:10.1029/2006GB002714.

Le Quéré, C., et al. (2007), Saturation of the Southern Ocean CO_2 sink due to recent climate change, *Science*, *316*, 1735–1738.

Lovenduski, N. S., and N. Gruber (2005), Impact of the Southern Annular Mode on Southern Ocean circulation and biology, *Geophys. Res. Lett.*, *32*, L11603, doi:10.1029/2005GL022727.

Marshall, G. J. (2003), Trends in the Southern Annular Mode from observations and reanalyses, *J. Clim.*, *16*, 4134–4143.

Marti, O., et al. (2006), The new IPSL climate system model:IPSL-CM4, *Note Poles Model. 26*, Inst. Pierre Simon Laplace, Paris.

Metzl, N. (2009), Decadal increase of ocean carbon dioxide in southern Indian Ocean surface waters (1991–2007), *Deep Sea Res., Part II*, doi:10.1016/j.dsr2.2008.12.007, in press.

Perlwitz, J., S. Pawson, R. L. Fogt, J. E. Nielsen, and W. D. Neff (2008), Impact of stratospheric ozone hole recovery on Antarctic climate, *Geophys. Res. Lett.*, *35*, L08714, doi:10.1029/2008GL033317.

Orr, J. C., et al. (2005), Anthropogenic ocean acidification over the twenty-first century and its impact on calcifying organisms, *Nature*, *437*, 681–686.

Randel, W. J., and F. Wu (2007), A stratospheric ozone profile data set for 1979–2005: Variability, trends, and comparisons with column ozone data, *J. Geophys. Res.*, *112*, D06313, doi:10.1029/2006JD007339.

Raven, J., et al. (2005), Ocean acidification due to increasing atmospheric carbon dioxide, policy document, R. Soc., London.

Riebesell, U., et al. (2000), Reduced calcification of marine plankton in response to increased atmospheric CO_2, *Nature*, *407*, 364–367.

Son, S.-W., et al. (2008), The impact of stratospheric ozone recovery on the Southern Hemisphere westery jet, *Science*, *320*, 1486–1489.

Song, Y., and W. A. Robinson (2004), Dynamical mechanisms for stratospheric influences on the troposphere, *J. Atmos Sci.*, *61*, 1711–1725.

Sunda, W. G., and S. A. Huntsman (1997), Interrelated influence or iron, light, and cell size on marine growth, *Nature*, *390*, 389–392.

Takahashi, T., et al. (2009), Climatological mean and decadal change in surface ocean pCO_2, and net sea-air CO_2 flux over the global oceans, *Deep Sea Res., Part II*, doi:10.1016/j.dsr2.2008.12.009, in press.

Timmerman, R., et al. (2005), On the representation of high latitude processes in the ORCA-LIM global coupled sea ice-ocean model, *Ocean Modell.*, *8*, 175–201.

Wanninkhof, R. (1992), Relationship between wind speed and gas exchange over the ocean, *J. Geophys. Res.*, *97*, 7373–7382.

L. Bopp, P. Cadule, and A. Tagliabue, LSCE, IPSL, CEA, UVSQ, CNRS, F-91191 Gif-sur-Yvette, France.

F. Codron, LMD, IPSL, UPMC, X, ENS, CNRS, F-75252 Paris, France.

A. Lenton and N. Metzl, LOCEAN, IPSL, UPMC, MHNH, IRD, CNRS, F-75005 Paris, France. (andrew.lenton@locean-ipsl.upmc.fr)

J. Le Sommer, LEGI, UJF, INPG, CNRS, F-38041 Grenoble, France.